immuno

MDPI

Article

EXT1 as an Independent Prognostic Biomarker in Breast Cancer: Its Correlation with Immune Infiltration and Clinicopathological Parameters

Amira Hossny [1,2], Hatem A. F. M. Hassan [3], Sherif Ashraf Fahmy [4,*], Hazem Abdelazim [5,6], Mahmoud Mohamed Kamel [7], Ahmed H. Osman [8] and Sherif Abdelaziz Ibrahim [1,*]

1 Department of Zoology, Faculty of Science, Cairo University, Giza 12613, Egypt; ahossny@msa.edu.eg
2 Faculty of Biotechnology, October University for Modern Sciences and Arts, Giza 12451, Egypt
3 Medway School of Pharmacy, University of Kent, Chatham Maritime, Kent ME4 4TB, UK; h.a.hassan@kent.ac.uk
4 Department of Pharmaceutics and Biopharmaceutics, University of Marburg, Robert-Koch-Str. 4, 35037 Marburg, Germany
5 Oncologic Pathology Department, National Cancer Institute, Cairo University, Cairo 11562, Egypt
6 Baheya Centre for Early Detection and Treatment of Breast Cancer, Cairo 11562, Egypt
7 Clinical Pathology Department, National Cancer Institute, Cairo University, Cairo 11562, Egypt
8 Department of Pathology, Faculty of Veterinary Medicine, Cairo University, Giza 12613, Egypt
* Correspondence: sheriffahmy@aucegypt.edu (S.A.F.); isherif@cu.edu.eg (S.A.I.)

Abstract: Exostosin 1 (EXT1) encodes a type II transmembrane glycosyltransferase residing in the endoplasmic reticulum and plays an essential role in the elongation of heparan sulfate chain biosynthesis. Additionally, EXT1 may act as an oncogene that could promote cell proliferation as well as cancer cell metastasis. Herein, we investigated EXT1's expression pattern and prognostic value in breast cancer, along with its immunological implications. Immunohistochemical staining of EXT1 was assessed in 85 breast cancer patients. Patients were categorized into molecular subtypes, namely luminal A, luminal B, and human epidermal growth factor receptor 2 (HER2), along with triple-negative breast cancer (TNBC). Correlations of EXT1 immunostaining with clinicopathological parameters were evaluated. Furthermore, the correlations of EXT1 expression with tumor immune infiltration and immune cell surface markers were assessed using TIMER. Moreover, survival analysis was conducted to reveal EXT1's prognostic value. EXT1 expression was markedly associated with the status of the estrogen receptor (ER), molecular subtypes, and recurrence status. In addition, high levels of EXT1 expression were associated with worse overall survival (OS) and relapse-free survival (RFS). Analysis of immune infiltration indicated that EXT1 expression was positively correlated with dendritic cells (DCs), macrophages, neutrophils, $CD4^+$ T cells, and $CD8^+$ T cells, although it showed a negative correlation with the tumor purity. Overall, this study suggests that the elevated EXT1 expression, particularly in TNBC, has a positive correlation with poor prognosis and with immune-infiltrated cells in breast cancer. Therefore, it may emerge as an independent prognostic biomarker, immunological marker, and potential future therapeutic target for the most aggressive TNBC subtype.

Keywords: exostosin 1 (EXT1); breast cancer; prognosis; immune infiltration

Academic Editor: Marcos López Hoyos

Received: 31 October 2024
Revised: 14 December 2024
Accepted: 17 December 2024
Published: 26 December 2024

Citation: Hossny, A.; Hassan, H.A.F.M.; Fahmy, S.A.; Abdelazim, H.; Kamel, M.M.; Osman, A.H.; Ibrahim, S.A. EXT1 as an Independent Prognostic Biomarker in Breast Cancer: Its Correlation with Immune Infiltration and Clinicopathological Parameters. *Immuno* **2025**, *5*, 1. https://doi.org/10.3390/immuno5010001

1. Introduction

Breast cancer constitutes a major worldwide health concern, diagnosed at a rate of over two million new cases each year and accounting for approximately 11.7% of all cancer cases. It is a major contributor to cancer-related mortality among women globally,

responsible for 6.9% of cancer-related deaths. The mortality rate among female breast cancer patients is greater in developing countries than in developed nations, with 15.0 deaths per 100,000 cases in developing countries, compared to 12.8 deaths per 100,000 cases in developed countries [1]. Breast cancer has long been categorized according to the clinicopathological features, including tumor size, stage, and lymph node involvement. This categorization has led to the classification being determined by whether the three surrogate molecular markers are present or absent, including estrogen receptors (ERs), progesterone receptors (PRs), and human epidermal growth factor receptor 2 (HER2). The fourth subtype is triple-negative breast cancer (TNBC), which lacks all three standard molecular markers [2,3]. Tumors are subsequently classified as luminal A (ER+, PR−/PR+, HER2−), luminal B (ER+, PR−/PR+, HER2+), HER2 (ER−, PR−, HER2+), and TNBC (ER−, PR−, HER2−) [4].

The extracellular matrix (ECM) is essential for cellular interactions and is rich in proteoglycans (PGs) and glycosaminoglycans (GAGs), forming a complex network that connects cells [5]. Among the ECM components, heparan sulfate PGs (HSPGs) are the most abundant [6]. HSPGs are comprised of a core protein with heparan sulfate (HS) chains that are attached via covalent bonds. They can be categorized differently according to the subcellular as well as cellular localization, the homology of the core protein, and their role [7]. HS can be described as a GAG chain that is anionic, long, and linear, as well as structurally composed of repetitive disaccharide molecules of N-acetyl-glucosamine and hexuronic acid components, which could be glucuronic acid or its C5 epimer, iduronic acid [8]. These units are extensively modified with various sulfate groups, leading to structures that are highly negatively charged [9]. In mammals, the following five genes have been identified: EXT1, EXT2, and three genes encoding EXT-like proteins; EXTL1, EXTL2, and EXTL3. The first phase of HS chain elongation is catalyzed by these EXT-like enzymes, which add β1,4-linked N-acetyl galactosamine to the expanding HS backbone. Both EXT1 and EXT2 encode glycosyltransferases that modify exogenous phytate and exhibit tumor-suppressing functions [10]. EXT1 is mapped to chromosome 8 and is responsible for encoding a type II transmembrane glycosyltransferase that resides within the endoplasmic reticulum. This enzyme plays a key role in the elongation stage of HS biosynthesis [11]. Previous in vitro studies have shown that both EXT1 and EXT2 exhibit transferase activities for glucuronic acid and N-acetyl-glucosamine [12,13]. EXT1 or EXT2 mutations highlight the crucial role of these enzymes in HS production, as they are linked to hereditary multiple exostoses (HME) development [14]. HSPGs are crucial for signal transduction, impacting processes such as cell migration, division, differentiation, and survival [15]. HSPGs also play crucial roles in pathological conditions, acting as key regulators of interactions between cancer cells and the ECM. Additionally, HSPGs could influence the behavior of the cancer cell and modify the tumor microenvironment (TME), affecting the progression of disease [16].

The TME comprises diverse cellular and molecular elements that aid in the advancement of cancer. Key components within the TME, including immune cells, extracellular matrix proteins, fibroblasts, and cytokines, are essential for driving tumor progression, invasion, and metastasis [17]. All of these elements work together in a complex manner through interactions between cells and the surrounding matrix to create an environment that promotes tumor growth [18,19]. Prior studies have demonstrated that dendritic cells (DCs), tumor-infiltrating lymphocytes (TILs), and tumor-associated macrophages (TAMs), along with tumor-associated neutrophils (TANs)and a variety of other cells, play significant roles in influencing tumor therapy outcomes and prognosis [20–22]. Effector immune cells infiltrating the TME can directly target and eliminate neoplastic cells presenting neoantigens on their surface, thereby inhibiting tumor progression [23]. Furthermore, $CD8^+$ T cells are vital in eliminating tumor cells by recognizing specific antigens presented by

MHC class I, while $CD4^+$ T cells help by releasing various effector cytokines. Although B cells make up a small portion of TILs, their presence is important for the development of TILs, which are clusters of lymphocytes within non-lymphoid tissues. The stroma of the breast cancer is characterized by the presence of these cells that are linked to high-grade tumors [24]. However, tumor cells utilize various immune evasion mechanisms that limit immune cell infiltration and disrupt their effector functions within the TME [25].

Previous studies have proposed that EXT1 could act as a tumor suppressor. EXT1 was initially identified as being epigenetically inactivated, leading to impaired HS, which is pivotal in promoting tumor initiation and progression [26]. Additionally, EXT1 expression is reduced in acute lymphoblastic leukemia (ALL) and associated with poorer survival outcomes [27]. Moreover, pro-tumorigenic signaling was suppressed by EXT1 in MV3 melanoma cells, emphasizing its relevance to chemosensitivity [28]. In contrast, other studies have found evidence supporting the role of EXT1 in tumor growth and malignancy. EXT1 has been suggested to act as an oncogene in tumors, promoting cell proliferation and influencing the WNT signaling pathway, which in turn enhances the migration of non-small cell lung carcinoma cell lines [29]. Furthermore, EXT1 has been reported to play a pro-tumorigenic role in a glioblastoma model. Knocking out EXT1 led to reduced cell proliferation in vitro and inhibited the growth of glioblastoma xenografts in mice by suppressing receptor tyrosine kinase activity [30]. Additionally, elevated EXT1 protein levels in ovarian cancer patients, compared to those who are therapy-sensitive, highlight its potential as a biomarker for predicting treatment response [31]. Thus, the overall role of EXT1 in tumor entities is controversial and remains poorly understood in breast cancer.

Therefore, the aim of this study was to examine the expression pattern and prognostic significance of EXT1, as well as the correlation between EXT1 expression with the clinicopathological parameters, along with the infiltration of immune cells in breast cancer.

2. Materials and Methods

2.1. Materials

EXT1 polyclonal antibody against EXT1 was purchased from (NOVUSBIO, Cat. NBP1-91875, Minneapolis, MN, USA). ER, PR, HER2 and Ki-67 targeting monoclonal antibodies were purchased from (Santa Cruz Biotechnology, San Diego, CA, USA). Mouse/Rabbit-Immuno Detector-HRP Detection system was purchased from (BIOSB, Cat. BSB 0001S, San Diego, CA, USA). All other chemicals were obtained from (Sigma-Aldrich, Dorset, UK).

2.2. Breast Cancer Tissue Samples

Formalin-fixed, paraffin-embedded (FFPE) tissue specimens were retrieved from a total of 85 patients with breast cancer (mean age of 52.92 years) between January 2018 and December 2021, after obtaining ethical approval from the Baheya Research Ethics Committee, Baheya Centre for Early Detection and Treatment of Breast Cancer (Cairo, Egypt) (Ref. 202210240048). The criteria for inclusion were as follows: female patients aged $\geq$18 years with confirmed diagnosis of invasive breast cancer according to the WHO classification of breast tumors [32]; stages I–III; immunohistochemically stained for ER, PR, and HER2; patients who were administered with neoadjuvant or adjuvant chemotherapy; those who were subjected to curative surgery via breast-conserving surgery (BCS) or modified radical mastectomy (MRM); and cases with complete clinical data and available archived paraffin blocks.

Patients who initially exhibited stage IV metastatic disease, incomplete medical records, loss of follow up data, or insufficient paraffin blocks were excluded. To determine the molecular subtype, immunohistochemical staining for ER, PR, and HER2, as well as Ki67 was performed. The patient cohort consisting of 85 breast cancer cases was classified

into subtypes as follows: luminal A (34 cases), luminal B (18 cases), HER2+ (14 cases), and TNBC (19 cases).

2.3. Immunohistochemical Staining

The FFPE tissue specimens were sequentially sectioned at 3–5 µm thickness and mounted on slides that were coated with positively charged poly-L-lysine. Breast cancer tissue samples were assessed to verify the initial diagnosis and to evaluate the expression levels of ER, PR, HER2, and Ki-67 (Figure 1).

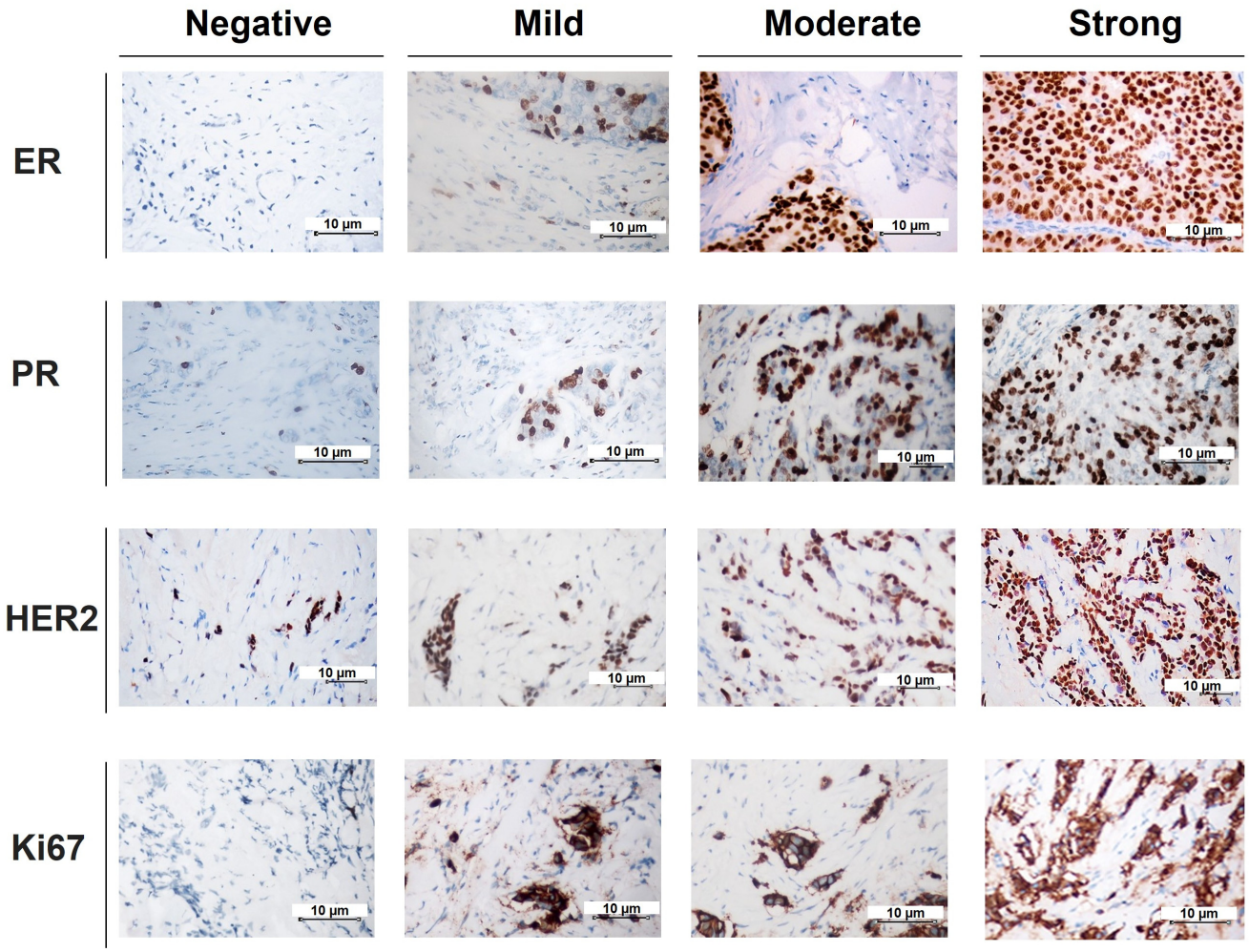

Figure 1. Representative images of immunostaining for ER, PR, HER2, and Ki67 breast cancer sections. The sections were stained using immunohistochemical protocol. The panels show varying intensities of staining for each marker ER, PR, HER2, and Ki67. The staining patterns are classified as negative, mild, moderate, and strong, as indicated by the respective columns. Images were captured at 40× magnification, and scale bar represents 10 µm for all images.

As previously described [33,34], the selected sections were deparaffinized in xylene for 15 min then gradually rehydrated in alcohol (100%, 80%, 70%, and 50%) for 10 min each, followed by rinsing with deionized water for 5 min. Heat induction was used to perform antigen retrieval with 10 mM sodium citrate buffer (pH 6.0) and then maintained for 10 min at a sub-boiling temperature. Afterwards, the slides were kept at room temperature for a duration of 30 min and subsequently washed by immersion in distilled water for a duration of 5 min. Blocking of endogenous peroxidase activity was carried out through the incubation of tissue sections with hydrogen peroxide (3%) for 5 min in methanol, followed by two washes using distilled water. For permeabilization, sections were rinsed two times

for 10 min each using a permeabilization buffer with 1% animal serum. Non-specific binding in tissue sections was blocked through an incubation with (5%) animal serum in PBS-T for a duration of 30 min at room temperature. The primary antibody against EXT1 diluted 1:100 in PBS with 1% animal serum was applied to the sections and incubated at room temperature for 2 h and then at 4 °C overnight under humid conditions. The sections were then washed twice with animal serum (1%) in PBS, 10 min each. Detection was carried out using Mouse/Rabbit-Immuno Detector-HRP Detection system (Cat. BSB 0001S-BioSB). The first step involved adding the immunodetector biotinylated secondary antibody link for 10 min, then proceeding with three rinses with PBS, 10 min each. The second detection step involved adding the HRP label for 10 min, followed by three rinses with PBS lasting 10 min each. Subsequently, a substrate–chromogen mixture (3,3′-diaminobenzidine tetrahydrochloride [DAB] in a chromogenic substrate buffer) was applied for a duration of 10 min. The counterstaining of the tissue sections was carried out using hematoxylin for 30 s and rinsed with PBS. The tissue sections were dehydrated by immersing the slides in 95% ethanol two times for 10 s each, then immersing them in 100% ethanol for 10 s each, and finally treating them with xylene twice for 10 s each. Mounting of the tissue sections was then carried out using dibutylphthalate polystyrene xylene (DPX) as the mounting medium. Negative controls involved the same procedure with no application of the primary antibody.

2.4. Immunohistochemical Detection of EXT1 and Scoring

Tissue sections were histologically examined with a light microscope (Olympus CX31, Dublin, Ireland) at 40× magnification to identify positive immunostaining. The average percentage of cells exhibiting positivity was determined utilizing Fiji ImageJ Software version 1.2, (Baltimore, MD, USA) [35]. The scoring criteria for EXT1 expression were based on the extent (E) as well as the intensity (I) of EXT1 staining. Each parameter was assigned a value from 0 to 3. For the extent of staining, a score of 0 was given to samples without detectable EXT1 staining, 1 when staining was detected in less than 30% of the tumor cells showed staining, 2 at when staining was detected in 30–60% of tumor cells being stained, and 3 at over 60% of tumor cells displaying staining. The scoring system for intensity was as follows: 0: no staining; 1: mild staining; 2: moderate staining; and 3: strong staining. The mean values for both extent and intensity were calculated from triplicate samples for each tissue section. The staining score for each sample was calculated by multiplying the mean E and I values, resulting in a score from 0 to 9. Following the method represented by Klein et al., the average of all obtained scores was calculated. Subsequently, tumor specimens were then categorized into either low or high EXT1 expression groups based on the median value for EXT1 expression. This classification was subsequently used to construct a contingency table and survival curves [36].

2.5. EXT1 mRNA Expression Analysis Using UALCAN

The UALCAN database (https://ualcan.path.uab.edu/index.html), accessed on 12 December 2024, was employed to analyze the EXT1 mRNA expression levels in normal breast tissues in comparison to the major molecular subtypes of breast cancer [37].

2.6. Single-Cell Analysis for Immune Cell Infiltration Using TIMER

We utilized the (TIMER) database (https://cistrome.shinyapps.io/timer/), that was accessed on 28 August 2024, to examine the influence of EXT1 expression on the levels of immune cell infiltration through the application of the gene module [38]. The analysis encompassed various immune cells, including the DCs, macrophages, neutrophils, B cells, and $CD4^+$ T and $CD8^+$ T cells. Furthermore, we employed TIMER to examine the correlations between EXT1 expression and immune cell markers. Tumor purity is crucial in

assessing immune infiltration levels in tumor samples and was considered in the genomic analysis of tumor samples.

2.7. Statistical Analysis

Statistical analysis of the data was performed using SPSS, version 26, IBM Inc., Armonk (NY, USA), with $p < 0.05$ demonstrating statistical significance. All p-values were determined as two-tailed. Mean ± SD was used to represent the normally distributed data, while median and interquartile ranges were both used for non-normally distributed data. Associations between breast cancer subtypes and clinicopathological parameters were examined using chi-squared tests, and the relationship between the EXT1 scores and the clinicopathological characteristics was assessed using linear-by-linear association. The Kruskal–Wallis test was employed to evaluate age differences among the subtypes breast cancer. Additionally, Kaplan–Meier survival curves along with log-rank tests were utilized in OS and RFS assessments, while Cox regression was employed in univariate and multivariate analyses.

3. Results

3.1. Clinicopathological Parameters of 85-Patient Cohort

The patients' clinicopathological characteristics, including hormone receptor status, tumor type, histological grade, tumor stage, nodal stage, metastasis status, adjuvant chemotherapy, and recurrence are depicted in Table 1. IHC staining was carried out for ER, PR, HER2, and Ki67 to subclassify the breast cancer patients into molecular subtypes (Figure 1). Representative images depicting EXT1 immunostaining are shown in Figure 2. Normal breast tissue sections did not show observable EXT1 staining (Supplementary Figure S1). Elevated EXT1 expression predominantly displayed a distinct cytoplasmic and membrane staining pattern, and no nuclear staining was observed in the 85-patient cohort.

Table 1. Clinicopathological parameters of the 85-patient cohort.

Parameters	Total (n = 85) %	Luminal A (n = 34) %	Luminal B (n = 18) %	HER2 (n = 14) %	TNBC (n = 19) %	*p* Value
Age (year, mean ± SD)	52.92 ± 11.71	54.06 ± 12.1	50.78 ± 9.84	50.50 ± 7.65	54.74 ± 14.94	0.825
Menopausal status						
Pre-menopausal	46 (54.1%)	18 (52.9%)	12 (66.7%)	8 (57.1%)	8 (42.1%)	0.526
Post-menopausal	39 (45.9%)	16 (47.1%)	6 (33.3%)	6 (42.9)	11 (57.9%)	
ER						
Negative	36 (42.35%)	2 (5.9%)	1 (5.6%)	14 (100%)	18 (100%)	**<0.001**
Positive	49 (57.65%)	32 (94.1%)	17 (94.4%)	0 (0%)	0 (0%)	
PR						
Negative	35 (41.2%)	1 (2.9%)	1 (5.6%)	14 (100%)	19 (100%)	**<0.001**
Positive	50 (58.8%)	33 (97.1%)	17 (94.4%)	0 (0%)	0 (0%)	
HER2						
Negative	55 (64.7%)	34 (100%)	2 (11.1%)	0 (0%)	19 (100%)	0.156
Positive	30 (35.3%)	0 (0%)	16 (88.9%)	14 (100%)	0 (0%)	
Tumor type						
Lobular	5 (5.9%)	1 (2.9%)	0 (0%)	0 (0%)	4 (21.1%)	**0.001**
Ductal	66 (77.6%)	23 (67.6%)	12 (85.7%)	16 (88.9%)	15 (78.9%)	
Mixed/Other	14 (16.5%)	10 (29.4%)	2 (14.3%)	2 (11.1%)	0 (0%)	
Histological Grade						
I/II	57 (67.1%)	26 (76.5%)	14 (77.8%)	8 (57.1%)	9 (47.4%)	**0.020**
III	28 (32.9%)	8 (23.5%)	4 (22.2%)	6 (42.9%)	10 (52.6%)	

Table 1. *Cont.*

Parameters	Total (n = 85) %	Luminal A (n = 34) %	Luminal B (n = 18) %	HER2 (n = 14) %	TNBC (n = 19) %	*p* Value
T						
T1	44 (51.8%)	20 (58.8%)	10 (55.6%)	6 (42.9%)	8 (42.1%)	0.344
T2	22 (25.9%)	9 (26.5%)	4 (22.2%)	2 (14.3%)	7 (36.8%)	
T3	8 (9.4%)	2 (5.9%)	0 (0%)	2 (14.3%)	4 (21.1%)	
T4	11 (12.9%)	3 (8.8%)	4 (22.2%)	4 (28.6%)	0 (0%)	
N						
N0	54 (63.5%)	22 (64.7%)	8 (44.4%)	10 (71.4%)	14 (73.7%)	0.382
N1	16 (18.8%)	6 (17.6%)	4 (22.2%)	2 (14.3%)	4 (21.1%)	
N2	9 (10.6%)	6 (17.6%)	2 (11.1%)	0 (0%)	1 (5.3%)	
N3	6 (7.1%)	0 (0%)	4 (22.2%)	2 (14.3%)	0 (0%)	
M						
Negative	64 (75.3%)	22 (64.7%)	18 (100%)	13 (92.9%)	11 (57.9%)	0.907
Positive	21 (24.7%)	12 (35.3%)	0 (0%)	1 (7.1%)	8 (42.1%)	
Adjuvant chemotherapy						
No	43 (50.6%)	14 (41.2%)	16 (88.9%)	11 (78.6%)	2 (10.5%)	0.142
Yes	42 (49.4%)	20 (58.8%)	2 (11.1%)	3 (21.4%)	17 (89.5%)	
Recurrence						
No	52 (61.2%)	20 (58.8%)	18 (100%)	13 (92.9%)	1 (5.3%)	**0.003**
Yes	33 (38.8%)	14 (41.2%)	0 (0%)	1 (7.1%)	18 (94.7%)	

The Kruskal–Wallis test utilized to evaluate significant age variations, while linear-by-linear association was used to analyze all other parameters statistically. TNBC: Triple-negative breast cancer, HER2: Human epidermal growth factor receptor type 2, ER Estrogen receptor; PR: Progesterone receptor; T: Tumor; N: Nodal status; M: Metastasis. Significant *p*-values are indicated in bold.

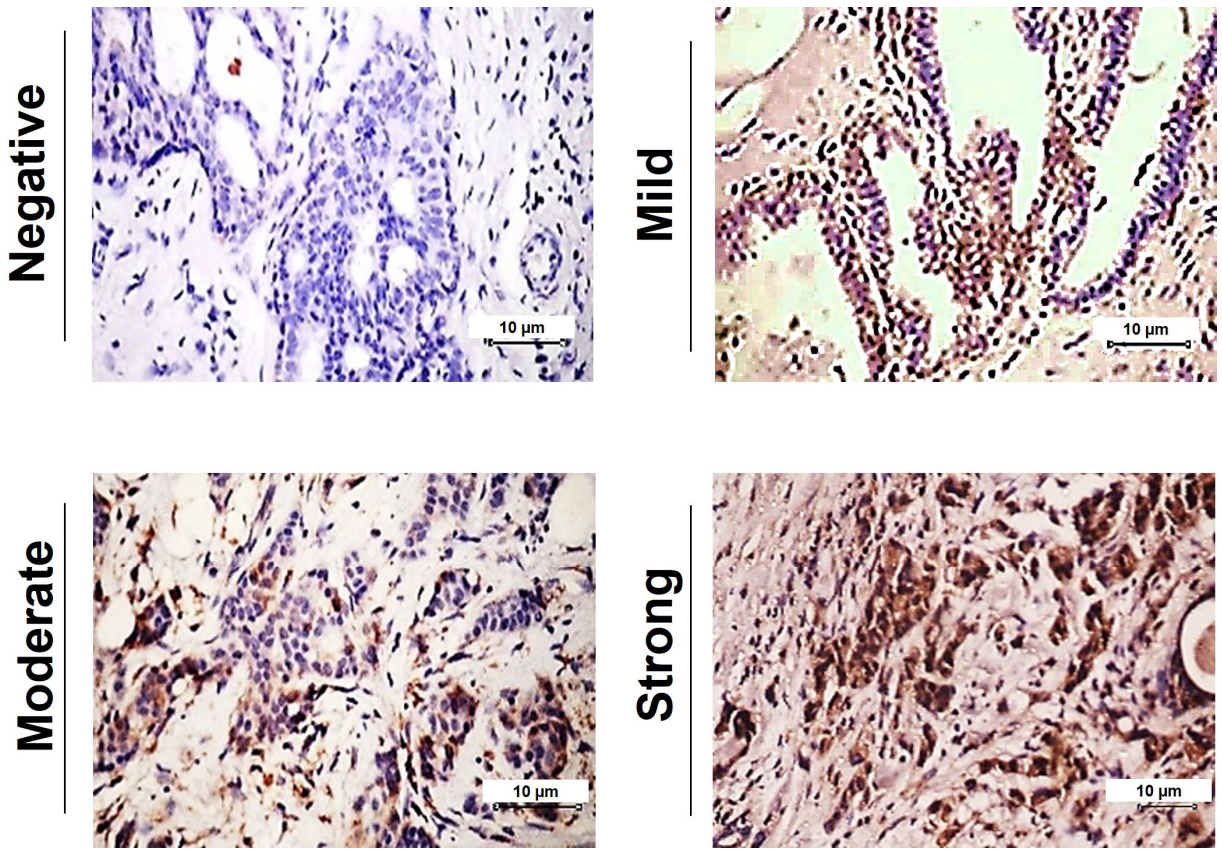

Figure 2. Representative images of the intensity of immunostaining for EXT1 in human breast cancer sections. The sections were stained using immunohistochemical protocol. The panels show varying intensities of staining for EXT1. Two main criteria were used for assessment: staining intensity and

the proportion of cell area showing positive staining (%), assessed by Fiji Image J software. The intensity of staining was assessed using a scoring system ranging from 0 to 3, with no staining represented by a score of 0, mild staining represented by a score of 1, moderate staining represented by a score of 2, and strong staining represented by a score of 3. Images captured by 40× magnification, scale bars = 10 μm.

As detailed in Table 2, 76.5% of luminal A patients showed a positive expression of EXT1, along with 77.78% of luminal B patients, 85.71% of HER2 patients, and 100% of TNBC patients. The immunohistochemical staining of EXT1 was expressed as low score (≤1) and high score (>1).

Table 2. Positive and negative EXT1 scoring in breast cancer patients with different molecular subtypes.

Molecular Subtype	Negative (n, Score = 0) (%)	Positive (n, Score = 1–9) (%)	Total
Luminal A	8 (23.5%)	26 (76.5%)	34
Luminal B	4 (22.2%)	14 (77.8%)	18
Her2	2 (14.3%)	12 (85.7%)	14
TNBC	0 (0%)	19 (100%)	19

HER2 (Human Epidermal Growth Factor Receptor 2); and TNBC (triple-negative breast cancer).

3.2. High EXT1 Expression Is Significantly Associated with ER Negativity, TNBC Subtype, and Recurrence

As depicted in Table 3, EXT1 was found to be significantly associated with an ER-negative status (p = 0.003), with 61.1% of the ER-negative tumors displaying a higher EXT1 score (>1) compared to 38.9% of the ER-positive tumors. However, no notable significant associations were detected between the EXT1 expression and either PR or HER2 status. According to the examined molecular subtypes, an elevated EXT1 expression level was significantly associated with TNBC (p = 0.008). Specifically, 38.9% of TNBC cases showed high EXT1 scores > 1, whereas only 11.1% of cases with luminal B had a high EXT1 expression score. Interestingly, breast cancer recurrence association was observed with high EXT1 expression (p = 0.005), with 55.3% of recurrent cases exhibiting high EXT1 expression scores compared to 44.7% of non-recurrent cases with high EXT1 scores. No notable significant associations were detected between EXT1 expression and other clinicopathological data.

Table 3. Association between EXT1 immunostaining expression scoring and clinicopathological parameters.

Parameter	Total n (%)	Low EXT1 Score (≤1) n (%)	High EXT1 Score (>1) n (%)	p Value
Age				
≤50	42 (49.4%)	24 (45.3%)	18 (56.3%)	0.33
>50	43 (50.6%)	29 (54.7%)	14 (43.8%)	
Menopausal status				
Pre-menopausal	58 (68.2%)	38 (71.7%)	20 (62.5%)	0.38
Post-menopausal	27 (31.8%)	15 (28.3%)	12 (37.5%)	
ER				
Negative	36 (42.4%)	14 (28.6%)	22 (61.1%)	**0.003**
Positive	49 (57.6%)	35 (71.4%)	14 (38.9%)	
PR				
Negative	35 (41.2%)	21 (39.6%)	14 (43.8%)	0.71
Positive	50 (58.8%)	32 (60.4%)	18 (56.3%)	

Table 3. *Cont.*

Parameter	Total n (%)	Low EXT1 Score (≤1) n (%)	High EXT1 Score (>1) n (%)	*p* Value
HER2				
Negative	55 (64.7%)	33 (62.3%)	22 (68.8%)	0.547
Positive	30 (35.3%)	20 (37.7%)	10 (31.3%)	
Tumor type				
Lobular	5 (5.9%)	3 (5.7%)	2 (6.3%)	
Ductal	66 (77.6%)	40 (75.5%)	26 (81.3%)	0.503
Mixed/Other	14 (16.5%)	10 (18.9%)	4 (12.5%)	
Grade				
I/II	57 (67.1%)	35 (66.0%)	22 (68.8%)	0.798
III	28 (32.9%)	18 (34.0%)	10 (31.3%	
T				
T1	44 (51.8%)	26 (54.2%)	18 (48.6%)	
T2	23 (27.1%)	8 (16.7%)	15 (40.5%)	0.135
T3	8 (9.4%)	4 (8.3%)	4 (10.8%)	
T4	10 (11.8%)	10 (20.8%)	0 (0%)	
N				
N0	54 (63.5%)	29 (61.7%)	25 (65.8%)	
N1	14 (16.5%)	6 (12.8%)	8 (21.1%)	0.164
N2	11 (12.9%)	6 (12.8%)	5 (13.2%)	
N3	6 (7.1%)	6 (12.8%)	0 (0%)	
M				
Negative	73 (85.9%)	45 (84.9%)	28 (87.5%)	0.741
Positive	12 (14.1%)	8 (15.1%)	4 (12.5%)	
Molecular subtype				
Luminal A	34 (40%)	22 (44.9%)	12 (33.3%)	
Luminal B	18 (21.2%)	14 (28.6%)	4 (11.1%)	**0.008**
HER2	14 (16.5%)	8 (16.3%)	6 (16.7%)	
TNBC	19 (22.4%)	5 (10.2%)	14 (38.9%)	
Recurrence				
No	52 (61.2%)	35 (74.5%)	17 (44.7%)	**0.005**
Yes	33 (38.8%)	12 (25.5%)	21 (55.3%)	

The classification as low EXT1 score or high EXT1 score was determined by the median score detected. EXT1: Exostosin. Significant *p*-values are indicated in bold.

In addition to utilizing TMA, we applied the scoring system to assess data dispersion based on classical breast cancer markers. Our analysis revealed that the ER-negative patients exhibited significantly higher EXT1 scores compared to the ER-positive patients ($p = 0.0127$) (Figure 3). No significant differences were detected for PR and HER2 status, which may be due to the small sample size. Regarding tumor subtypes, luminal B displayed lower EXT1 scores, while TNBC exhibited significantly elevated mean EXT1 scores ($p = 0.029$) (Figure 3).

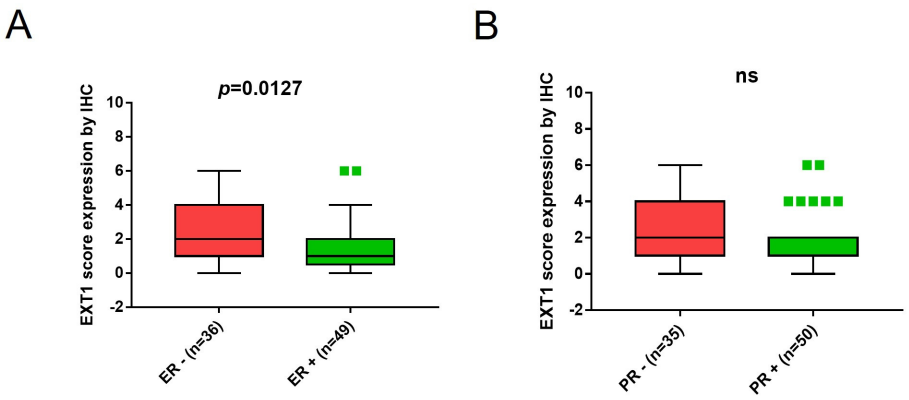

Figure 3. *Cont.*

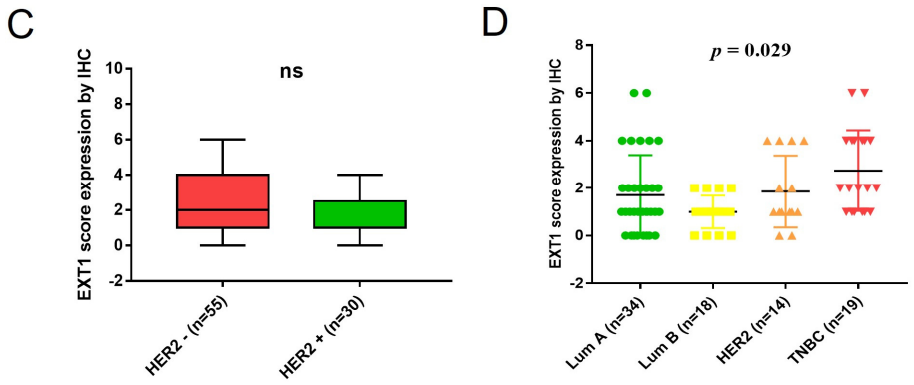

Figure 3. EXT1 expression scoring dispersion according to (**A**) ER (**B**) PR, (**C**) HER2, and (**D**) different molecular subtypes of breast cancer. ns denotes for not significant.

3.3. High EXT1 Expression Is Positively Correlated with Breast Cancer Poor Prognosis

To assess the EXT1 expression's prognostic significance in breast cancer patients, we examined EXT1 expression using Kaplan–Meier survival curves. Following a median of 35 months of follow-up, both OS and RFS were evaluated. The findings showed that patients who exhibited higher EXT1 expression had significantly poorer OS and RFS ($p = 0.016$, $p = 0.027$), respectively (Figure 4).

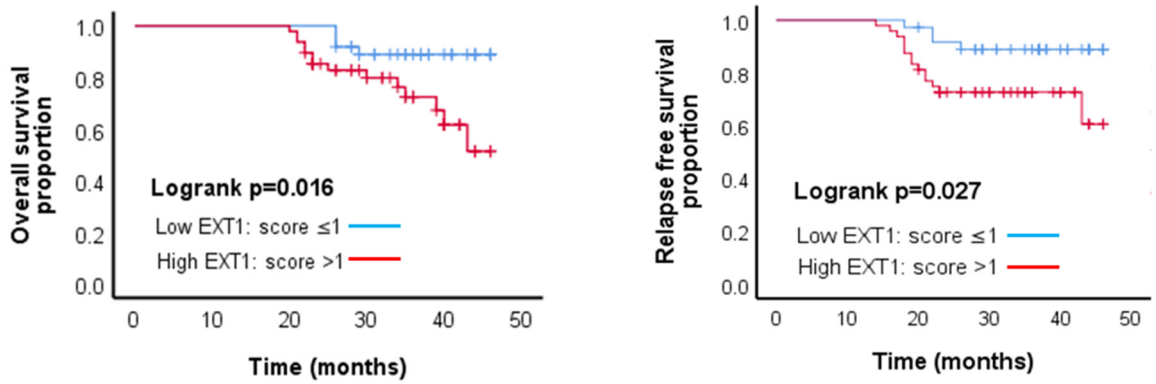

(**A**) (**B**)

Figure 4. The Kaplan–Meier survival curves of (**A**) OS and (**B**) RFS of breast cancer cases according to EXT1 expression scores.

3.4. EXT1 Expression Independently Predicts Prognosis in Breast Cancer Cases

To assess the influence of high EXT1 expression on clinical outcomes, both univariate as well as multivariate Cox regression analyses were conducted. In the univariate analysis, EXT1 expression levels were significantly associated with both poorer OS and RFS ($p = 0.025$, HR = 3.578, CI 1.172–10.919; $p = 0.038$, HR = 3.262, CI 1.069–9.954), respectively (Table 4). Additionally, PR status was markedly associated with poor OS ($p = 0.028$, HR = 3.517, CI 1.142–10.837), while for RFS, the analysis indicated no significance ($p = 0.069$, HR = 2.82, CI 0.923–8.62) (Table 4).

Table 4. Univariate analysis for OS and RFS of variables associated with survival rates in breast cancer patients.

Variable	Univariate OS Analysis		Univariate RFS Analysis	
	Hazard Ratio (95% CI)	***p* Value**	**Hazard Ratio (95% CI)**	***p* Value**
EXT1 score (≤1 vs. >1)	3.578 (1.172–10.919)	**0.025**	3.262 (1.069–9.954)	**0.038**
ER status (negative vs. positive)	1.932 (0.717–5.204)	0.193	1.622 (0.605–4.344)	0.336

Table 4. *Cont.*

Variable	Univariate OS Analysis		Univariate RFS Analysis	
	Hazard Ratio (95% CI)	***p* Value**	**Hazard Ratio (95% CI)**	***p* Value**
PR status (negative vs. positive)	3.517 (1.142–10.837)	**0.028**	2.82 (0.923–8.62)	0.069
HER2 status (negative vs. positive)	0.311 (0.09–1.077)	0.065	0.35 (0.101–1.209)	0.097
T (T1 vs. T2, T3, T4)	1.01 (0.397–2.569)	0.983	0.882 (0.348–2.235)	0.791
N (negative vs. positive)	1.611 (0.602–4.306)	0.342	1.251 (0.479–3.268)	0.647
M (negative vs. positive)	1.242 (0.358–4.302)	0.733	1.291 (0.374–4.462)	0.686

CI: Confidence interval. Significant *p*-values are indicated in bold.

Furthermore, multivariate analysis via Cox regression confirmed that EXT1 expression was an unfavorable independent factor associated with both OS and RFS ($p = 0.027$, HR = 3.649, CI 1.158–11.494; $p = 0.039$, HR = 3.318, CI 1.068–10.339), respectively (Table 5). Considering ER status, HER2 status, PR status, tumor stage, nodal status, and metastasis, no significant associations were found in the multivariate analysis, suggesting that these factors do not have a notable impact on OS or RFS in our patient cohort.

Table 5. Multivariate cox regression analysis for both OS and RFS of variables associated with survival rates in breast cancer patients.

Variable	Multivariate OS Analysis		Multivariate RFS Analysis	
	Hazard Ratio (95% CI)	***p* Value**	**Hazard Ratio (95% CI)**	***p* Value**
EXT1 score (≤1 vs. >1)	3.649 (1.158–11.494)	**0.027**	3.318 (1.068–10.339)	**0.039**
ER status (negative vs. positive)	0.811 (0.179–3.668)	0.785	0.51 (0.113–2.308)	0.382
PR status (negative vs. positive)	3.734 (0.725–19.234)	0.115	4.63 (0.879–24.381)	0.071
HER2 status (negative vs. positive)	0.293 (0.08–1.077)	0.065	0.356 (0.095–1.324)	0.123
T (T1 vs. T2, T3, T4)	1.068 (0.373–3.06)	0.902	0.906 (0.333–2.468)	0.847
N (negative vs. positive)	1.719 (0.576–5.136)	0.332	1.088 (0.383–3.093)	0.874
M (negative vs. positive)	0.58 (0.151–2.223)	0.427	0.836 (0.221–3.165)	0.792

CI: Confidence interval. Significant *p*-values are indicated in bold.

3.5. Correlation Between EXT1 mRNA Expression and Immune Cells Infiltration in Breast Cancer

The mRNA expression of EXT1 was found to be significantly higher in normal breast tissues compared to breast cancer tissues of the luminal and HER2 molecular subtypes (Supplementary Figure S2). In contrast, TNBC tissues demonstrated higher EXT1 mRNA expression than both normal breast tissues and other molecular subtypes. Immune cells within the breast cancer microenvironment could significantly influence patients' survival [39]. Accordingly, an assessment of the correlation between EXT1 mRNA expression in breast cancer and immune cell infiltration is of considerable significance. We assessed the EXT1 mRNA expression's correlation with immune cell infiltration in breast cancer, as well as across different breast cancer subtypes, including basal, HER2-enriched, and luminal subtypes, using the TIMER database (accessed on 28 August 2024).

Our single-cell analysis showed that EXT1 mRNA expression exhibited a positive correlation with the infiltration of B cells (r = 0.11, $p = 5.80e{-}04$), $CD8^+$ T cells (r = 0.31, $p = 3.60e{-}23$), $CD4^+$ T cells (r = 0.168, $p = 1.50e{-}07$), macrophages (r = 0.269, $p = 1.00e{-}17$), neutrophils (r = 0.34, $p = 3.68e{-}27$), and DCs (r = 0.312, $p = 5.48e{-}23$). Conversely, *EXT1* mRNA expression demonstrated a negative correlation with tumor purity (r = −0.131, $p = 3.39e{-}05$) (Figure 5A).

Specifically in the basal subtype, EXT1 mRNA expression demonstrated a negative correlation with tumor purity (r = −0.09, $p = 3.13e{-}01$) and exhibited a positive correlation with the infiltration of B cells (r = 0.064, $p = 4.78e{-}01$), $CD8^+$ T cells (r = 0.176, $p = 5.21e{-}02$), $CD4^+$ T cells (r = 0.211, $p = 1.96e{-}02$), macrophages (r = 0.23, $p = 9.19e{-}03$), neutrophils (r = 0.285, $p = 2.56e{-}03$), and DCs (r = 0.259, $p = 5.41e{-}03$) (Figure 5B). In the

HER2 subtype, EXT1 mRNA expression showed a negative correlation with tumor purity (r = −0.089, p = 5.01e−01), as well as with B cells (r = −0.097, p = 4.71e−01), $CD8^+$ T cells (r = −0.116, p = 3.91e−01), $CD4^+$ T cells (r = −0.14, p = 2.93e−01), neutrophils (r = −0.009, p = 9.45e−01), and DCs (r = −0.028, p = 8.36e−01). However, it did not demonstrate a significant correlation with the macrophages (r = 0.163, p = 2.21e−01) (Figure 5C). In the luminal subtype, EXT1 mRNA expression demonstrated a negative correlation with tumor purity (r = −0.182, p = 1.88e−05), while it exhibited positive correlations with B cells (r = 0.097, p = 2.45e−02), $CD8^+$ T cells (r = 0.313, p = 1.19e−13), $CD4^+$ T cells (r = 0.211, p = 8.47e−07), macrophages (r = 0.382, p = 3.13e−20), neutrophils (r = 0.362, p = 5.06e−18), and DCs (r = 0.349, p = 9.61e−17) (Figure 5D).

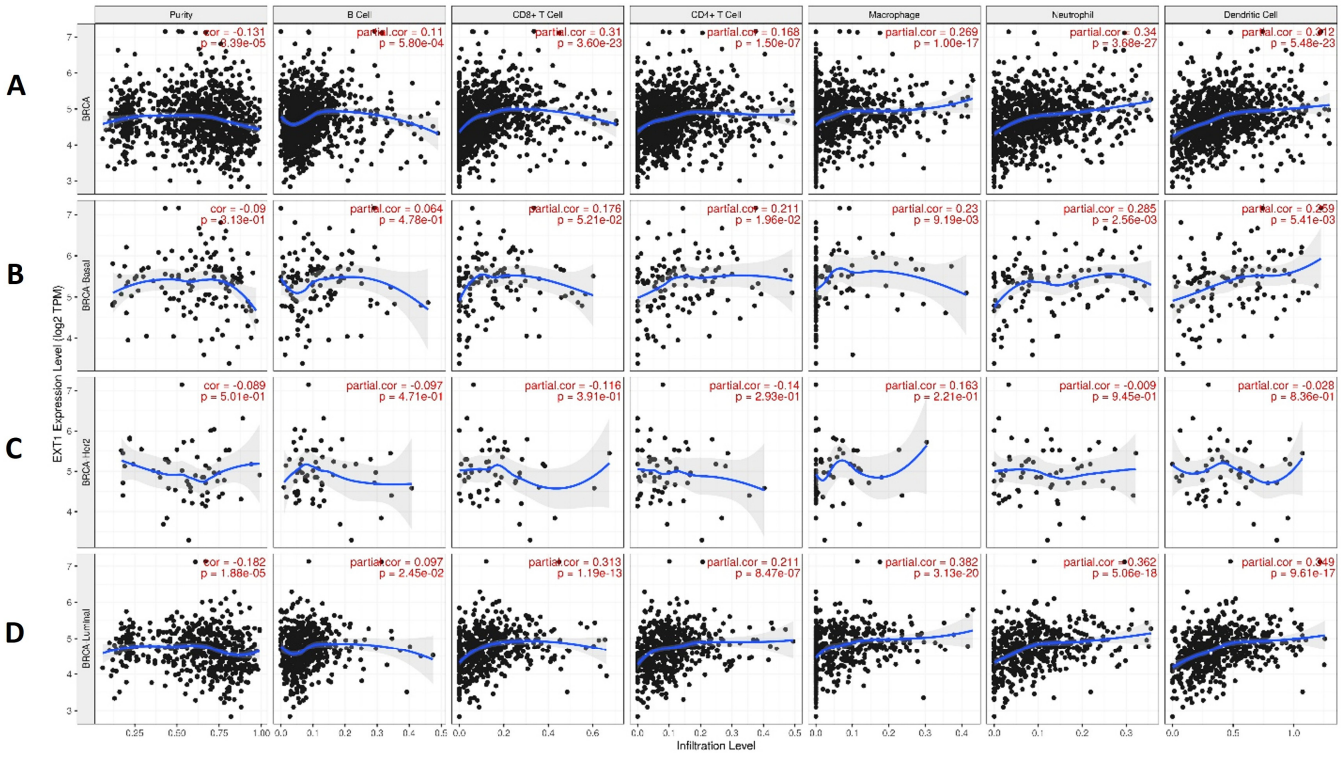

Figure 5. The correlation between EXT1 mRNA expression and levels of immune cell infiltration, as analyzed by TIMER database. (**A**) whole breast cancer; (**B**) Basal subtype; (**C**) Her2 subtype; and (**D**) luminal subtypes. Cor: r value of Spearman's correlation; Purity: adjusted correlation for tumor purity.

3.6. Correlation Between the EXT1 mRNA Expression and Immune Cell Markers

The TIMER database was used in the assessment EXT1 mRNA expression correlation with immune cell markers. Numerous immune cells, namely DCs, neutrophils, natural killer (NK) cells, TAMs, M1/M2 macrophages, monocytes, B cells, and $CD8^+$ T cells were identified and examined based on their unique characteristics. Furthermore, various functional T cell subsets were investigated, including regulatory T cells (Treg), T helper cell subsets, and T follicular helper (Tfh) cells. Upon adjusting for tumor purity, the TIMER assessment revealed significant correlations between EXT1 mRNA expression and 35 out of 47 immune cell markers (Table 6).

Table 6. Correlation of EXT1 mRNA with immune cell type markers within the TME.

Cell Type	Gene Marker	None		Tumor Purity	
		Cor.	*p*	Cor.	*p*
B cell	CD19	0.037	2.23e−01	−0.023	4.61e−01
	MS4A1	0.064	3.46e−02 *	0.007	8.04e−01
	CD38	0.213	1.06e−12 ***	0.189	1.96e−09 ***
$CD8^+$ T cell	CD8A	0.099	1.101e−03 **	0.052	9.91e−02
	CD8B	0.107	3.89e−04	0.07	2.82e−02 *
Tfh cell	CXCR5	0.08	8.03e−03 **	0.02	5.24e−01
	ICOS	0.247	9.81e−17 ***	0.222	1.22e−12 ***
	BCL-6	0.204	8.06e−12 ***	0.191	1.08e−09 ***
Th1 cell	IL12RB2	0.328	4.87e−29 ***	0.323	1.35e−25 ***
	IL27RA	0.147	8.98e−07 ***	0.106	8.21e−04 ***
	TBX21	0.125	3.10e−05 ***	0.076	1.71e−02 *
Th2 cell	CCR3	0.141	2.56e−06 ***	0.11	5.30e−04 ***
	STAT6	−0.03	3.18e−01	−0.045	1.54e−01
	GATA3	−0.303	1.00e−24 ***	−0.288	2.24e−20 ***
Th9 cell	TGFBR2	0.296	1.02e−23 ***	0.275	1.18e−18 ***
	IRF4	0.201	1.79e−11 ***	0.163	2.36e−07 ***
	SPI1	0.15	5.95e−07 ***	0.112	3.85e−04 ***
Th17 cell	IL-21R	0.272	3.69e−20 ***	0.244	5.47e−15 ***
	IL-23R	0.193	1.08e−10 ***	0.182	7.16e−09 ***
	STAT3	0.292	4.66e−23 ***	0.288	1.74e−20 ***
Th22 cell	CCR10	−0.116	1.11e−04 ***	−0.16	3.69e−07 ***
	AHR	0.31	6.35e−26 ***	0.299	5.31e−22 ***
Treg cell	FOXP3	0.218	2.59e−13 ***	0.188	2.51e−09 ***
	CCR8	0.302	1.37e−24 ***	0.283	8.14e−20 ***
	IL2RA	0.352	2.42e−33 ***	0.344	4.25e−29 ***
Exhausted T cell	PD-1	0.09	0.002e−03 ***	0.046	1.49e−01
	CTLA4	0.204	8.97e−1	0.174	3.44e−08 ***
Macrophage	CD68	0.284	6.93e−22 ***	0.277	6.62e−19 ***
	ITGAM	0.221	1.17e−13 ***	0.185	4.51e−09 ***
	TGFB1	0.12	6.48e−05 ***	0.064	4.37e−02 *
M1	NOS2	0.242	3.94e−16 ***	0.24	1.96e−14 ***
	ROS1	0.327	6.69e−29 ***	0.329	1.57e−26 ***
M2	ARG1	0.056	6.28e−02	0.054	8.69e−02
	MRC1	0.302	1.20e−24 ***	0.291	6.66e−21 ***
TAM	HLA-G	0.06	4.52e−02 *	0.036	2.55e−01
	CD80	0.375	4.37e−38 ***	0.364	1.49e−32 ***
Monocyte	CD14	0.178	2.61e−09 ***	0.149	2.25e−06 ***
	FCGR3A	0.302	1.39e−24 ***	0.283	1.02e−19 ***
	FCGR3B	0.206	4.70e−12 ***	0.214	9.14e−12 ***

Table 6. *Cont.*

Cell Type	Gene Marker	None		Tumor Purity	
		Cor.	*p*	Cor.	*p*
NK	XCL1	0.16	1.01e−07 ***	0.133	2.59e−05 ***
	KIR3DL1	0.139	3.89e−06 ***	0.12	1.55e−04 ***
	CD7	0.081	7.13e−03 **	0.031	3.28e−01
Neutrophil	FUT4	0.383	9.91e−40 ***	0.38	1.81e−35 ***
	MPO	0.158	1.43e−07 ***	0.141	7.60e−06 ***
DC	CD1C	0.035	2.46e−01	−0.025	4.24e−01
	THBD	0.069	2.22e−02 *	0.023	4.61e−01
	CCR7	0.061	4.15e−02 *	0.011	7.31e−01

Cor: r value of Spearman's correlation; Purity: adjusted correlation for tumor purity. * $p < 0.05$, ** $p < 0.01$, *** $p < 0.001$.

4. Discussion

Although there have been significant advancements in cancer treatment, many patients continue to experience recurrences and/or develop resistance to therapy, leading to elevated death rates [40]. Consequently, the identification of new diagnostic, prognostic, and therapeutic targets remain essential. EXT1 has been the subject of multiple studies, highlighting its relevance in various biological processes and its potential role in cancer progression [29,41,42]. Previous studies reported the dysregulated expression of EXT1 in various cancer types, for instance, hepatocellular carcinoma (HCC) and ALL [41,43].

Our study has revealed that EXT1 is significantly overexpressed in breast cancer patients, specifically in TNBC. Furthermore, the elevated EXT1 expression is associated with poor prognosis, and tumor recurrence. Hence, EXT1 expression could act as a key regulator of the aggressiveness of breast cancer. Conversely, another study showed that lower EXT1 expression is associated with poorer patient survival in ALL [27], suggesting that EXT1 functions in tumor entities are context dependent.

Further, increased EXT1 immunostaining was found to be associated with ER-negative breast cancer. These findings align with the study by Julien et al., who reported elevated EXT1 mRNA expression in ER-negative breast tumors, a subtype that exhibits a higher incidence of metastasis [44]. Various studies suggest that EXT1 may function as an oncogene in tumors, potentially driving cell proliferation and influencing the WNT signaling pathway that could promote the non-small cell lung cancer migration [29]. As Wnt signaling is known to be involved in regulating cancer stem cells [45,46], this further supports our finding of the association of the high EXT1 expression with tumor recurrence. Furthermore, it has been reported that EXT1's function cannot be compensated by other EXT family members, such as EXT2. In an in vitro study, knocking out EXT1 decreased cell proliferation and suppressed glioblastoma growth in mice by weakening the activity of receptor tyrosine kinases, suggesting a pro-tumorigenic role for EXT1 [30]. Together, this supports the oncogenic role of elevated EXT1 levels in breast cancer.

TNBC is widely recognized for its excessive relapses and worse prognosis, with a survival rate of 8–16% over 5 years, which is lower than that of other breast cancer types [47]. Moreover, as a result of ER, PR, and HER2 absence, all TNBC cases are unresponsive to hormone therapy or anti-HER2 treatment [48]. Hence, our findings of the highest EXT1 immunostaining scores observed in TNBC in comparison to the other molecular subtypes underscore the potential of EXT1 as a therapeutic target. Nonetheless, further investigations are crucial for us to understand the mechanisms behind the elevated EXT1 expression, which might result in a wider investigation of its therapeutic potential and reinforce its

role as an oncogenic marker in breast tissue, potentially serving as a surrogate marker for predicting the clinical outcomes.

Moreover, the data presented herein suggest that various factors, including EXT1 levels and PR status, can significantly influence both OS and RFS in our patient cohort. However, the influence of these factors may vary based on the patient population and the methods used, such as IHC. Furthermore, the multivariate analysis suggests that EXT1 levels emerge as an independent prognostic factor in breast cancer.

Immune cells infiltration can significantly impact cancer development, progression, as well as metastasis [49]. Additionally, immune cells have also been recognized as significant prognostic indicators in breast cancer [50]. The interplay between cancer cells and the TME can either hinder or promote disease progression. Immune cells within tumors can suppress growth by targeting and eliminating immunogenic cancer cells. However, they may also facilitate the development of tumor resistance to therapy by altering tumor immunogenicity and selecting tumor clones that drive immune exhaustion [51]. In this context, a strong correlation has been detected between EXT1 expression and the infiltration of $CD8^+$ T cells, $CD4^+$ T cells, neutrophils, and DCs in head and neck squamous cell carcinoma [52]. In the present study, we extended this knowledge about the correlation that could exist between EXT1 expression and the immune cells in the breast cancer microenvironment, where EXT1 was correlated with B cells, $CD8^+$ T cells, $CD4^+$ T cells, neutrophils, macrophages, and DCs.

Our analysis demonstrated that EXT1 mRNA expression was found to be correlated with neutrophils. This aligns with a study by Xiang et al., reporting that elevated neutrophil count in breast cancer patients was associated with poorer overall survival [53]. Additionally, our analysis shows that EXT1 is crucial in modulating tumor immunity and may contribute to establishing an immune suppressive setting that enables tumor cells to evade immune surveillance, thereby promoting malignant progression. These findings are supported by our examination of the correlation between EXT1 and the immune cell-related markers in breast cancer. EXT1 expression exhibited a positive correlation with TGFB1 and the other immune cells' markers that contribute to immune suppression. The critical role that EXT1 plays in the TME as well as macrophage polarization was further validated through a study suggesting that TGFB1 could serve as a key immune suppressive molecule within the TME [54]. Additionally, another study demonstrated that EXT1 expression plays an essential role in immune response, affecting lymphocyte recruitment in endothelial cells in a murine model of contact hypersensitivity when EXT1 expression was lacking, resulting in impaired chemokine presentation [55]. Furthermore, Tregs were found to be abundant in breast cancer tissue than in normal tissue, and their presence could be associated with higher tumor grade, lymph node positivity, and reduced overall and recurrence-free survival [56,57]. This aligns with our findings that reveal a strong correlation between EXT1 mRNA expression and FOXP3, CCR8, and IL2RA. As databases are refined, the correlation between EXT1 mRNA expression and immune cell infiltration may evolve. Refined data classification supported by growing resources may strengthen the validity of the results. Nevertheless, future studies should focus on assessing the reliability of the reported findings.

5. Conclusions

In conclusion, EXT1 is elevated in TNBC and is associated with tumor recurrence. Further EXT1 expression is correlated with poor OS, RFS, and the immunosuppressive TME. Therefore, EXT1 emerges as an independent prognostic indicator and potential therapeutic target for TNBC. However, further studies are needed to decipher the precise molecular mechanisms contributing to elevated EXT1 expression levels in breast cancer.

Supplementary Materials: The following supporting information can be downloaded at: https://www.mdpi.com/article/10.3390/immuno5010001/s1. Figure S1. Representative image of immunostaining of EXT1 in normal breast tissue. The section was stained using immunohistochemical protocol. Image was captured at 40× magnification, and the scale bar represents 10 μm; Figure S2. EXT1 mRNA expression levels in normal breast tissues and major molecular subtypes of breast cancer using UALCAN (http://ualcan.path.uab.edu/) (accessed on 13 December 2024). *** $p < 0.001$.

Author Contributions: Conceptualization, A.H. and S.A.I.; methodology, A.H., H.A.F.M.H., M.M.K., A.H.O. and S.A.I.; software, A.H., H.A.F.M.H., A.H.O. and S.A.I.; validation, A.H., M.M.K., A.H.O. and S.A.I.; formal analysis, A.H., H.A.F.M.H., M.M.K., A.H.O. and S.A.I.; investigation, A.H., M.M.K., A.H.O. and S.A.I.; resources, A.H., H.A., M.M.K., A.H.O. and S.A.I.; data curation, A.H., H.A., M.M.K., A.H.O. and S.A.I.; writing—original draft preparation, A.H., H.A.F.M.H., S.A.F., M.M.K., A.H.O. and S.A.I.; writing—review and editing, A.H., H.A.F.M.H., S.A.F., M.M.K., A.H.O. and S.A.I.; visualization, A.H., M.M.K., A.H.O. and S.A.I.; supervision, M.M.K., A.H.O. and S.A.I.; project administration, M.M.K., A.H.O. and S.A.I.; Funding acquisition, S.A.F. All authors have read and agreed to the published version of the manuscript.

Funding: Sherif Ashraf Fahmy acknowledges the financial support and sponsorship received from the Alexander von Humboldt Foundation, Germany.

Institutional Review Board Statement: The study was conducted in accordance with the Declaration of Helsinki and approved by Baheya Research Ethics Committee, Baheya Centre for Early Detection and Treatment of Breast Cancer, Cairo, Egypt (Ref. 202210240048, 24 October 2022).

Informed Consent Statement: Informed consent was obtained from all subjects involved in the study.

Data Availability Statement: Study data will be made available upon reasonable request.

Conflicts of Interest: The authors declare no conflicts of interest.

References

1. Sung, H.; Ferlay, J.; Siegel, R.L.; Laversanne, M.; Soerjomataram, I.; Jemal, A.; Bray, F. Global cancer statistics 2020: GLOBOCAN estimates of incidence and mortality worldwide for 36 cancers in 185 countries. *CA A Cancer J. Clin.* **2021**, *71*, 209–249. [CrossRef] [PubMed]
2. Tsang, J.Y.; Gary, M.T. Molecular classification of breast cancer. *Adv. Anat. Pathol.* **2020**, *27*, 27–35. [CrossRef]
3. Waks, A.G.; Winer, E.P. Breast cancer treatment: A review. *JAMA* **2019**, *321*, 288–300. [CrossRef]
4. Cheang, M.C.; Martin, M.; Nielsen, T.O.; Prat, A.; Voduc, D.; Rodriguez-Lescure, A.; Ruiz, A.; Chia, S.; Shepherd, L.; Ruiz-Borrego, M. Defining breast cancer intrinsic subtypes by quantitative receptor expression. *Oncologist* **2015**, *20*, 474–482. [CrossRef] [PubMed]
5. Vallet, S.D.; Clerc, O.; Ricard-Blum, S. Glycosaminoglycan–protein interactions: The first draft of the glycosaminoglycan interactome. *J. Histochem. Cytochem.* **2021**, *69*, 93–104. [CrossRef] [PubMed]
6. Hassan, N.; Greve, B.; Espinoza-Sánchez, N.A.; Götte, M. Cell-surface heparan sulfate proteoglycans as multifunctional integrators of signaling in cancer. *Cell Signal.* **2021**, *77*, 109822. [CrossRef] [PubMed]
7. Iozzo, R.V.; Schaefer, L. Proteoglycan form and function: A comprehensive nomenclature of proteoglycans. *Matrix Biol.* **2015**, *42*, 11–55. [CrossRef]
8. Lindahl, U.; Couchman, J.; Kimata, K.; Esko, J.D. Proteoglycans and sulfated glycosaminoglycans. In *Essentials of Glycobiology*; Cold Spring Harbor Laboratory Press: Cold Spring Harbor, NY, USA, 2017.
9. Esko, J.D.; Selleck, S.B. Order out of chaos: Assembly of ligand binding sites in heparan sulfate. *Annu. Rev. Biochem.* **2002**, *71*, 435–471. [CrossRef]
10. Busse-Wicher, M.; Wicher, K.B.; Kusche-Gullberg, M. The extostosin family: Proteins with many functions. *Matrix Biol.* **2014**, *35*, 25–33. [CrossRef]
11. McCormick, C.; Leduc, Y.; Martindale, D.; Mattison, K.; Esford, L.; Dyer, A.; Tufaro, F. The putative tumour suppressor EXT1 alters the expression of cell-surface heparan sulfate. *Nat. Genet.* **1998**, *19*, 158–161. [CrossRef] [PubMed]
12. Senay, C.; Lind, T.; Muguruma, K.; Tone, Y.; Kitagawa, H.; Sugahara, K.; Lidholt, K.; Lindahl, U.; Kusche-Gullberg, M. The EXT1/EXT2 tumor suppressors: Catalytic activities and role in heparan sulfate biosynthesis. *EMBO Rep.* **2000**, *1*, 282–286. [CrossRef] [PubMed]

13. Busse, M.; Kusche-Gullberg, M. In vitro polymerization of heparan sulfate backbone by the EXT proteins. *J. Biol. Chem.* **2003**, *278*, 41333–41337. [CrossRef] [PubMed]
14. Cheung, P.K.; McCormick, C.; Crawford, B.E.; Esko, J.D.; Tufaro, F.; Duncan, G. Etiological point mutations in the hereditary multiple exostoses gene EXT1: A functional analysis of heparan sulfate polymerase activity. *Am. J. Hum. Genet.* **2001**, *69*, 55–66. [CrossRef]
15. Li, J.-P.; Kusche-Gullberg, M. Heparan sulfate: Biosynthesis, structure, and function. *Int. Rev. Cell Mol. Biol.* **2016**, *325*, 215–273. [PubMed]
16. Faria-Ramos, I.; Poças, J.; Marques, C.; Santos-Antunes, J.; Macedo, G.; Reis, C.A.; Magalhães, A. Heparan sulfate glycosaminoglycans: (Un)Expected allies in cancer clinical management. *Biomolecules* **2021**, *11*, 136. [CrossRef] [PubMed]
17. Li, J.J.; Tsang, J.Y.; Tse, G.M. Tumor microenvironment in breast cancer—Updates on therapeutic implications and pathologic assessment. *Cancers* **2021**, *13*, 4233. [CrossRef]
18. Baghban, R.; Roshangar, L.; Jahanban-Esfahlan, R.; Seidi, K.; Ebrahimi-Kalan, A.; Jaymand, M.; Kolahian, S.; Javaheri, T.; Zare, P. Tumor microenvironment complexity and therapeutic implications at a glance. *Cell Commun. Signal.* **2020**, *18*, 59. [CrossRef]
19. Butti, R.; Kumar, T.V.; Nimma, R.; Banerjee, P.; Kundu, I.G.; Kundu, G.C. Osteopontin signaling in shaping tumor microenvironment conducive to malignant progression. In *Tumor Microenvironment: Advances in Experimental Medicine and Biology*; Springer: Cham, Switzerland, 2021; pp. 419–441.
20. Mahmoud, S.M.; Paish, E.C.; Powe, D.G.; Macmillan, R.D.; Grainge, M.J.; Lee, A.H.; Ellis, I.O.; Green, A.R. Tumor-infiltrating $CD8^+$ lymphocytes predict clinical outcome in breast cancer. *J. Clin. Oncol.* **2011**, *29*, 1949–1955. [CrossRef] [PubMed]
21. Broz, M.L.; Binnewies, M.; Boldajipour, B.; Nelson, A.E.; Pollack, J.L.; Erle, D.J.; Barczak, A.; Rosenblum, M.D.; Daud, A.; Barber, D.L. Dissecting the tumor myeloid compartment reveals rare activating antigen-presenting cells critical for T cell immunity. *Cancer Cell* **2014**, *26*, 638–652. [CrossRef] [PubMed]
22. Zhang, Y.; Cheng, S.; Zhang, M.; Zhen, L.; Pang, D.; Zhang, Q.; Li, Z. High-infiltration of tumor-associated macrophages predicts unfavorable clinical outcome for node-negative breast cancer. *PLoS ONE* **2013**, *8*, e76147. [CrossRef] [PubMed]
23. Burugu, S.; Asleh-Aburaya, K.; Nielsen, T.O. Immune infiltrates in the breast cancer microenvironment: Detection, characterization and clinical implication. *Breast Cancer* **2017**, *24*, 3–15. [CrossRef]
24. Zhang, Q.; Wu, S. Tertiary lymphoid structures are critical for cancer prognosis and therapeutic response. *Front. Immunol.* **2023**, *13*, 1063711. [CrossRef]
25. Binnewies, M.; Roberts, E.W.; Kersten, K.; Chan, V.; Fearon, D.F.; Merad, M.; Coussens, L.M.; Gabrilovich, D.I.; Ostrand-Rosenberg, S.; Hedrick, C.C. Understanding the tumor immune microenvironment (TIME) for effective therapy. *Nat. Med.* **2018**, *24*, 541–550. [CrossRef] [PubMed]
26. Ropero, S.; Setien, F.; Espada, J.; Fraga, M.F.; Herranz, M.; Asp, J.; Benassi, M.S.; Franchi, A.; Patino, A.; Ward, L.S. Epigenetic loss of the familial tumor-suppressor gene exostosin-1 (EXT1) disrupts heparan sulfate synthesis in cancer cells. *Hum. Mol. Genet.* **2004**, *13*, 2753–2765. [CrossRef]
27. Liu, N.-w.; Huang, X.; Liu, S.; Lu, Y. EXT1, regulated by MiR-665, promotes cell apoptosis via ERK1/2 signaling pathway in acute lymphoblastic leukemia. *Med. Sci. Monit. Int. Med. J. Exp. Clin. Res.* **2019**, *25*, 6491. [CrossRef] [PubMed]
28. Pfeifer, V.; Weber, H.; Wang, Y.; Schlesinger, M.; Gorzelanny, C.; Bendas, G. Exostosin 1 knockdown induces chemoresistance in MV3 melanoma cells by upregulating JNK and MEK/ERK signaling. *Int. J. Mol. Sci.* **2023**, *24*, 5452. [CrossRef]
29. Kong, W.; Chen, Y.; Zhao, Z.; Zhang, L.; Lin, X.; Luo, X.; Wang, S.; Song, Z.; Lin, X.; Lai, G. EXT1 methylation promotes proliferation and migration and predicts the clinical outcome of non-small cell lung carcinoma via WNT signalling pathway. *J. Cell. Mol. Med.* **2021**, *25*, 2609–2620. [CrossRef] [PubMed]
30. Ohkawa, Y.; Wade, A.; Lindberg, O.R.; Chen, K.Y.; Tran, V.M.; Brown, S.J.; Kumar, A.; Kalita, M.; James, C.D.; Phillips, J.J. Heparan sulfate synthesized by Ext1 regulates receptor tyrosine kinase signaling and promotes resistance to EGFR inhibitors in GBM. *Mol. Cancer Res.* **2021**, *19*, 150–161. [CrossRef] [PubMed]
31. Butt, T.; Cerantonio, A.; Cristiani, C.; Greco, M.; Foti, D.; Migliozzi, S.; Mignogna, C.; De Marco, C.; Viglietto, G. The role of Exostosin Glycosyltransferase 1 (EXT1) in ovarian cancer. In Proceedings of the 4th International Electronic Conference on Cancers, Online, 6–8 March 2024.
32. Tan, P.H.; Ellis, I.; Allison, K.; Brogi, E.; Fox, S.B.; Lakhani, S.; Lazar, A.J.; Morris, E.A.; Sahin, A.; Salgado, R. The 2019 WHO classification of tumours of the breast. *Histopathology* **2020**, *77*, 181–185. [CrossRef] [PubMed]
33. Ismail, Y.; Zakaria, A.-S.; Allam, R.; Götte, M.; Ibrahim, S.A.; Hassan, H. Compartmental Syndecan-1 (CD138) expression as a novel prognostic marker in triple-negative metaplastic breast cancer. *Pathol. Res. Pract.* **2024**, *253*, 154994. [CrossRef] [PubMed]
34. Coulson-Thomas, V.J.; Gesteira, T.F.; Esko, J.; Kao, W. Heparan sulfate regulates hair follicle and sebaceous gland morphogenesis and homeostasis. *J. Biol. Chem.* **2014**, *289*, 25211–25226. [CrossRef]
35. Schindelin, J.; Arganda-Carreras, I.; Frise, E.; Kaynig, V.; Longair, M.; Pietzsch, T.; Preibisch, S.; Rueden, C.; Saalfeld, S.; Schmid, B. Fiji: An open-source platform for biological-image analysis. *Nat. Methods* **2012**, *9*, 676–682. [CrossRef]

36. Klein, M.; Vignaud, J.-M.; Hennequin, V.; Toussaint, B.; Bresler, L.; Plenat, F.; Leclere, J.; Duprez, A.; Weryha, G. Increased expression of the vascular endothelial growth factor is a pejorative prognosis marker in papillary thyroid carcinoma. *J. Clin. Endocrinol. Metab.* **2001**, *86*, 656–658. [CrossRef] [PubMed]
37. Chandrashekar, D.S.; Bashel, B.; Balasubramanya, S.A.H.; Creighton, C.J.; Ponce-Rodriguez, I.; Chakravarthi, B.V.; Varambally, S. UALCAN: A portal for facilitating tumor subgroup gene expression and survival analyses. *Neoplasia* **2017**, *19*, 649–658. [CrossRef] [PubMed]
38. Li, T.; Fan, J.; Wang, B.; Traugh, N.; Chen, Q.; Liu, J.S.; Li, B.; Liu, X.S. TIMER: A web server for comprehensive analysis of tumor-infiltrating immune cells. *Cancer Res.* **2017**, *77*, e108–e110. [CrossRef]
39. Zhang, W.; Lee, A.; Tiwari, A.K.; Yang, M.Q. Characterizing the Tumor Microenvironment and Its Prognostic Impact in Breast Cancer. *Cells* **2024**, *13*, 1518. [CrossRef] [PubMed]
40. Siegel, R.L.; Giaquinto, A.N.; Jemal, A. Cancer statistics, 2024. *CA A Cancer J. Clin.* **2024**, *74*, 12–49. [CrossRef]
41. Dong, S.; Wu, Y.; Yu, S.; Yang, Y.; Lu, L.; Fan, S. Increased EXT1 gene copy number correlates with increased mRNA level predicts short disease-free survival in hepatocellular carcinoma without vascular invasion. *Medicine* **2018**, *97*, e12625. [CrossRef]
42. Solaimuthu, B.; Khatib, A.; Tanna, M.; Karmi, A.; Hayashi, A.; Abu Rmaileh, A.; Lichtenstein, M.; Takoe, S.; Jolly, M.K.; Shaul, Y.D. The exostosin glycosyltransferase 1/STAT3 axis is a driver of breast cancer aggressiveness. *Proc. Natl. Acad. Sci. USA* **2024**, *121*, e2316733121. [CrossRef] [PubMed]
43. Daakour, S. Perturbations of Interactome Networks in Acute Lymphoblastic Leukaemia: Identification of EXT1 Tumor Suppressor as a Notch Pathway Regulator. Ph.D. Thesis, Université de Liège, Liège, Belgium, 2016.
44. Julien, S.; Ivetic, A.; Grigoriadis, A.; QiZe, D.; Burford, B.; Sproviero, D.; Picco, G.; Gillett, C.; Papp, S.L.; Schaffer, L. Selectin ligand sialyl-Lewis x antigen drives metastasis of hormone-dependent breast cancers. *Cancer Res.* **2011**, *71*, 7683–7693. [CrossRef] [PubMed]
45. Kumar Katakam, S.; Tria, V.; Sim, W.C.; Yip, G.W.; Molgora, S.; Karnavas, T.; Elghonaimy, E.A.; Pelucchi, P.; Piscitelli, E.; Ibrahim, S.A. The heparan sulfate proteoglycan syndecan-1 regulates colon cancer stem cell function via a focal adhesion kinase—Wnt signaling axis. *FEBS J.* **2021**, *288*, 486–506. [CrossRef]
46. Abdullah, A.R.; El-Din, A.M.G.; El-Mahdy, H.A.; Ismail, Y.; El-Husseiny, A.A. The crucial role of fascin-1 in the pathogenesis, metastasis, and chemotherapeutic resistance of breast cancer. *Pathol. Res. Pract.* **2024**, *254*, 155079. [CrossRef] [PubMed]
47. Almansour, N.M. Triple-negative breast cancer: A brief review about epidemiology, risk factors, signaling pathways, treatment and role of artificial intelligence. *Front. Mol. Biosci.* **2022**, *9*, 836417. [CrossRef] [PubMed]
48. Kaplan, H.G.; Malmgren, J.A. Impact of triple negative phenotype on breast cancer prognosis. *Breast J.* **2008**, *14*, 456–463. [CrossRef] [PubMed]
49. Sokratous, G.; Polyzoidis, S.; Ashkan, K. Immune infiltration of tumor microenvironment following immunotherapy for glioblastoma multiforme. *Hum. Vaccines Immunother.* **2017**, *13*, 2575–2582. [CrossRef]
50. Schnellhardt, S.; Erber, R.; Büttner-Herold, M.; Rosahl, M.-C.; Ott, O.J.; Strnad, V.; Beckmann, M.W.; King, L.; Hartmann, A.; Fietkau, R. Tumour-infiltrating inflammatory cells in early breast cancer: An underrated prognostic and predictive factor? *Int. J. Mol. Sci.* **2020**, *21*, 8238. [CrossRef]
51. Gonzalez, H.; Hagerling, C.; Werb, Z. Roles of the immune system in cancer: From tumor initiation to metastatic progression. *Genes Dev.* **2018**, *32*, 1267–1284. [CrossRef] [PubMed]
52. Wang, Y.; Huang, Y.; Zhu, H.; Guo, Z.; Cheng, J.; Zhang, C.; Zhong, M. Exostoisns (EXT1/2) in Head and Neck Cancers: An In Silico Analysis and Clinical Correlates. *Int. Dent. J.* **2024**, *74*, 446–453. [CrossRef]
53. Xiang, M.; Zhang, H.; Tian, J.; Yuan, Y.; Xu, Z.; Chen, J. Low serum albumin levels and high neutrophil counts are predictive of a poorer prognosis in patients with metastatic breast cancer. *Oncol. Lett.* **2022**, *24*, 1–9. [CrossRef] [PubMed]
54. Woo, S.-R.; Corrales, L.; Gajewski, T.F. Innate immune recognition of cancer. *Annu. Rev. Immunol.* **2015**, *33*, 445–474. [CrossRef]
55. Swart, M.; Troeberg, L. Effect of polarization and chronic inflammation on macrophage expression of heparan sulfate proteoglycans and biosynthesis enzymes. *J. Histochem. Cytochem.* **2019**, *67*, 9–27. [CrossRef]
56. Khaja, A.S.S.; Toor, S.M.; El Salhat, H.; Faour, I.; Haq, N.U.; Ali, B.R.; Elkord, E. Preferential accumulation of regulatory T cells with highly immunosuppressive characteristics in breast tumor microenvironment. *Oncotarget* **2017**, *8*, 33159. [CrossRef] [PubMed]
57. Saleh, R.; Elkord, E. FoxP3+ T regulatory cells in cancer: Prognostic biomarkers and therapeutic targets. *Cancer Lett.* **2020**, *490*, 174–185. [CrossRef]